Rare Metal Materials and Engineering
Volume 48, Issue 2, February 2019
Available online at www.rmme.ac.cn

Science Press

Cite this article as: Rare Metal Materials and Engineering, 2019, 48(2): 0411-0418.

ARTICLE

Microstructure Characteristics and Mechanical Properties of Cu Matrix Composites Containing Micro-B_4C/Nano-Ti Particulates

An Decheng, Wang Wenxian, Chen Hongsheng, Tan Minbo, Wang Miao

Shanxi Key Laboratory of Advanced Magnesium-based Materials, Taiyuan University of Technology, Taiyuan 030024, China

Abstract: Micro-B_4C/nano-Ti hybrid particulates reinforced copper matrix composites (CTBCs) were prepared by high energy ball milling (HEBM) and spark plasma sintering (SPS). The microstructures and morphologies were characterized by X-ray diffraction (XRD), optical microscopy (OM), and scanning electron microscopy (SEM) equipped with energy dispersive spectroscopy (EDS). The relative density and mechanical properties of the as-SPSed samples were also tested. The results demonstrate that there are uniformly distributed (B_4C+Ti) particles in the Cu matrix and a good interfacial bond between reinforcement and the Cu matrix. Besides, the interface bonding mechanism is metallurgical bonding and mechanical bonding. Mechanical properties (microhardness, tensile yield strength, ultimate tensile strength and elongation to fracture) of CTBCs are significantly improved in comparison to the pure copper, which is mainly due to the load transfer, grain refinement and thermal mismatch. Finally, the fracture surface of the tensile sample presents ductile fractures.

Key words: copper matrix composites; spark plasma sintering; high energy ball milling; interface bonding; mechanical properties

Particle reinforced copper matrix composites (PRCMCs) have been attracting tremendous attention from many scientists in recent years due to their excellent structural and functional properties such as high thermal and electrical conductivity, good corrosion resistance and superior mechanical properties. It makes PRCMCs exhibit considerable application potential in electrical and nuclear power industries[1]. Nowadays, various hard reinforcements in micro- and nano-size including SiC[2], Al_2O_3[3], TiC[4], TiN[5], TiB_2[6] and diamond[7] have been applied to enhance copper matrix composites (CMCs). Besides, a range of preparation processes have been successful in fabricating these materials in the past two decades, which mainly consist of casting, spray-forming, infiltration and powder metallurgy[8-10] etc. Unfortunately, in B_4C/Cu composites, the poor wettability between B_4C and copper matrix causes difficulties in preparation when a conventional method is employed[11]. As a result, there is limited report about copper boron carbide composites along with relevant technology studies.

Boron carbide is one of the three hardest ceramic materials in nature (next to diamond and cubic boron nitride). Moreover, B_4C is widely used as a particle reinforcement in metal matrix composites (MMCs) because of its low density (2.52 g/cm^3), relatively high thermal and chemical stability and low cost, especially attractive neutron absorption properties for nuclear power engineering (the isotope of boron known as ^{10}B has great thermal neutron absorption cross-section)[12]. On the other hand, copper and its alloys possess reasonably distinguished processability (due to the face-centered-cubic lattice structure). But nevertheless, the intrinsic poor yield strength restricts its extensive applications in crucial engineering areas, and thus it is significant to improve the physical-mechanical properties of CMCs by B_4C[13].

Due to the high surface activity, low sintering temperature and moderate chemical reaction degree, the nano-titanium powder is designed to be an interlayer material in order to

Received date: February 25, 2018
Foundation item: National Natural Science Foundation of China (51375328)
Corresponding author: Wang Wenxian, Ph. D., Professor, College of Materials Science and Engineering, Taiyuan University of Technology, Taiyuan 030024, P. R. China, Tel: 0086-351-6010076, E-mail: wangwenxian@tyut.edu.cn

improve the interfacial bonding of the Cu-B_4C system[14]. In this paper, we prepared Cu-Ti-B_4C composites (CT-BCs) by high energy ball milling (HEBM) and spark plasma sintering (SPS). This technique involves cold welding of micro-B_4C and nano-Ti hybrid reinforcement, particulate fracturing processes via HEBM and high-speed powder sintering. Accordingly, our purposes were: (1) to refine the interface bonding state between B_4C particle and Cu matrix via synthesis of (B_4C+Ti) coated particle during high energy ball milling; (2) to explore suitable parameters for ball milling and SPS processes, and (3) to investigate the influence of the volume fraction of micro-B_4C/nano-Ti hybrid reinforcement on the mechanical properties of the bulk Cu-composites. The results of mechanical properties measurements were associated with microstructural characterization to comprehend the strengthening mechanisms of the new CMC materials.

1 Experiment

In this work the starting materials included branching copper (99.7% purity and particle size of 38 μm, Fig.1e), B_4C (98.1% purity and average particle size of 8 μm, Fig.1c) and nano-sized active metal Ti powders of size <60 nm (99.8% purity, Fig.1d) used as the coated materials of B_4C particulates. Ball-milling was carried out mainly in two procedures to prepare Cu-Ti-B_4C composite powders. Firstly, B_4C and Ti powders (the volume ratio of B_4C/Ti is 3:2) were mixed by the HEBM process (QM-3B) at 1400 r/min and with a ball-to-powder weight ratio of 10:1 for 8 h (Fig.1a). 1 wt% stearic acid was used as process control agent so as to avoid adhesion of particulates to wall of the jar. After every 15 min, HEBM process was suspended to prevent agglomeration of particles owing to overheating. Then, copper with different volume fractions of (B_4C+Ti) hybrid reinforcement (1, 3 and 5vol%) underwent low energy ball milling (LEBM) in a planetary ball mill (MITR-QM-QX-2L). The ball to powder weight ratio was 5:1, the rotating speed was 200 r/min and the ball-milling was accomplished for 40 min to allow Cu-Ti-B_4C composite powders to hybridize homogeneously (Fig.1b). The HEBM and LEBM processes were protected in a high purity argon atmosphere.

After milling, the blended powders were directly transferred into a cylindrical graphite die and then consolidated in the SPS-331Lx system (Japan). Fig.2 shows the sample arrangement and schematic sketch of the SPS system. The shape of the samples was a disc with 30 mm in diameter and 5 mm in height. SPS process was conducted in a vacuum atmosphere (<10^{-1} Pa) under an applied pressure of 25 MPa. The heating rate was 100 °C/min up to 500 °C and then 70 °C /min up to the SPS sintering temperature of 700 °C. A holding time of 5 min at the maximum temperature was employed (Fig.3).

The phase composition of the as-milled powders and the as-SPSed specimens was determined through X-ray diffraction (XRD) using a Y-2000 type X-ray diffractometer (Cu-Kα radiation) with a 2θ range of 20°~80°, operating at 40 kV and 30 mA. A DMC2900 OM was used to study the distribution of reinforcements in copper matrix of bulk Cu-composites. A TESCAN MIRA3 LMH SEM equipped with an EDS attachment was employed to demonstrate the microstructures of the

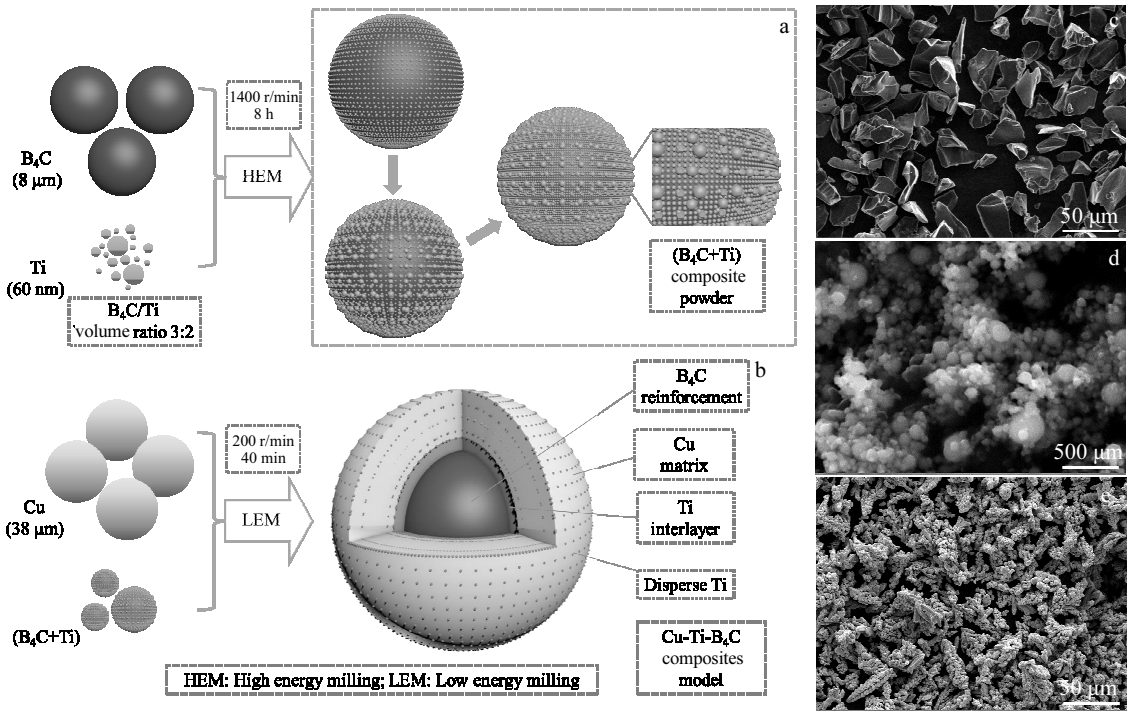

Fig.1 Schematic illustrations of design and preparation of Cu-Ti-B_4C composite powders (a, b) and SEM morphologies of as-received powders of B_4C (c), Ti (d) and Cu (e)

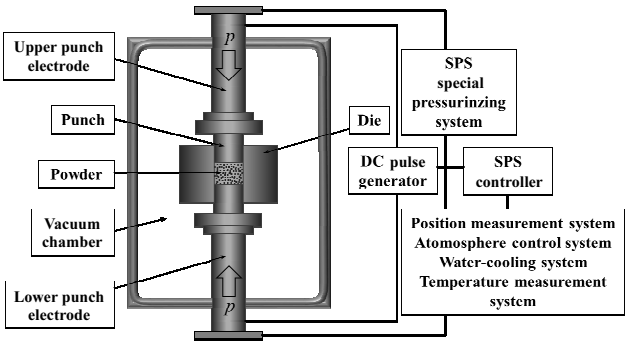

Fig.2 Schematic sketch of SPS system

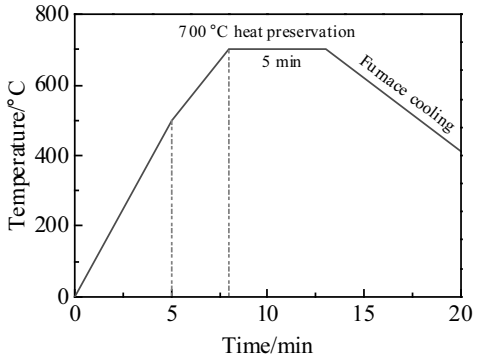

Fig.3 Schematic illustration of the sintering process of fabricating Cu-Ti-B_4C composites

sintered samples. The relative density of the composite samples was tested using Archimedes drainage method. Microhardness measurements were conducted on the as-polished specimens using HVS-1000A hardness testing machine under a load of 0.98 N and a dwell time of 15 s. Hardness values were obtained by averaging data of 7 repeatable readings. Tensile tests were carried out using DNS-200 universal testing machine at a crosshead speed of 0.5 mm/min. The fractured specimens under tensile loading of CTBCs were analysed by SEM.

2 Results and Discussion

2.1 Microstructural characteristics

Fig.4a presents the SEM micrographs of (B_4C+Ti) composite powder. It shows that nano-Ti particles adhere to surface of the micro-B_4C particles uniformly (after 8 h of HEBM). The agglomeration of nano-Ti appears owing to the inherent surface energy and cold welding of particles. Meanwhile, the micro-B_4C powders possess blunter edges and smaller particle size compared with the as-received B_4C powders. This can be attributed to ball-powder-ball/wall collisions during the ball milling process. That is to say, the continuous mechanical force causes flattening and fracturing of hard ceramic particles. The SEM micrograph of CTBCs is

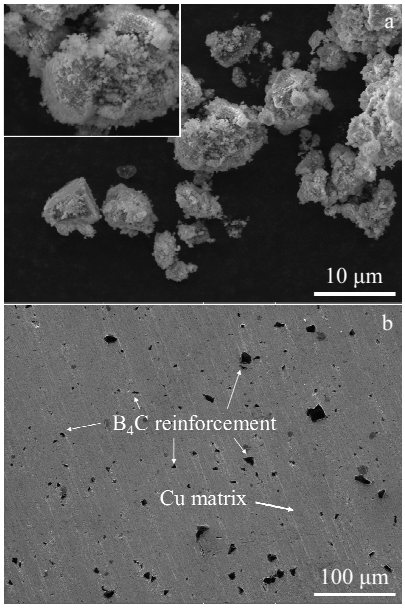

Fig.4 SEM micrographs of (B_4C+Ti) composite powder after 8 h of HEBM (a) and CTBCs sample fabricated by SPS at 700 °C (b)

shown in Fig.4b. The composite specimen is successfully sintered by SPS at 700 °C. Furthermore, there is no obvious defect in the microstructure of bulk samples and porosity is not fairly evident. CTBCs have a unique structure composed of Cu matrix, grey (B_4C+Ti) particles (with thicker coated layer) and bright black (B_4C+Ti) particles (with thinner coated layer). The thickness difference of (B_4C+Ti) coated particles mainly results from inhomogenous wear effect in the process of LEBM. Fig.5 shows the OM microstructures of CTBCs and B_4C/Cu composites with different percentages of reinforcement so as to study the distribution and morphology of second phases. As shown in Fig.5b~5e, micro-B_4C/nano-Ti hybrid reinforcements are uniformly distributed in the Cu matrix, with less agglomeration. At the same time, there are also the agglomerated particulates at a small scale as shown in Fig.5a, especially those that have higher volume fractions of particles, cause more seriously uneven distribution of reinforcements in the Cu matrix. The results of Fig.5 indicate that the procedure of HEBM enhances particle size refinement and this is beneficial to improving the toughness of Cu-materials[15].

The XRD patterns of ball milled powder are presented in Fig.6a. For (B_4C+Ti) powder, the XRD pattern is composed of prominent B_4C, Ti peaks and additional peaks corresponding to titanium compounds. In contrast, after the admixture of ball milled powder into the copper matrix, the X-ray peaks corresponding to B_4C and Ti are not conspicuously observed in the Cu-Ti-B_4C composite powder, which reveals only the Cu peaks. This is likely due to the comparatively low volume fraction of second phases, resulting in decreased intensity.

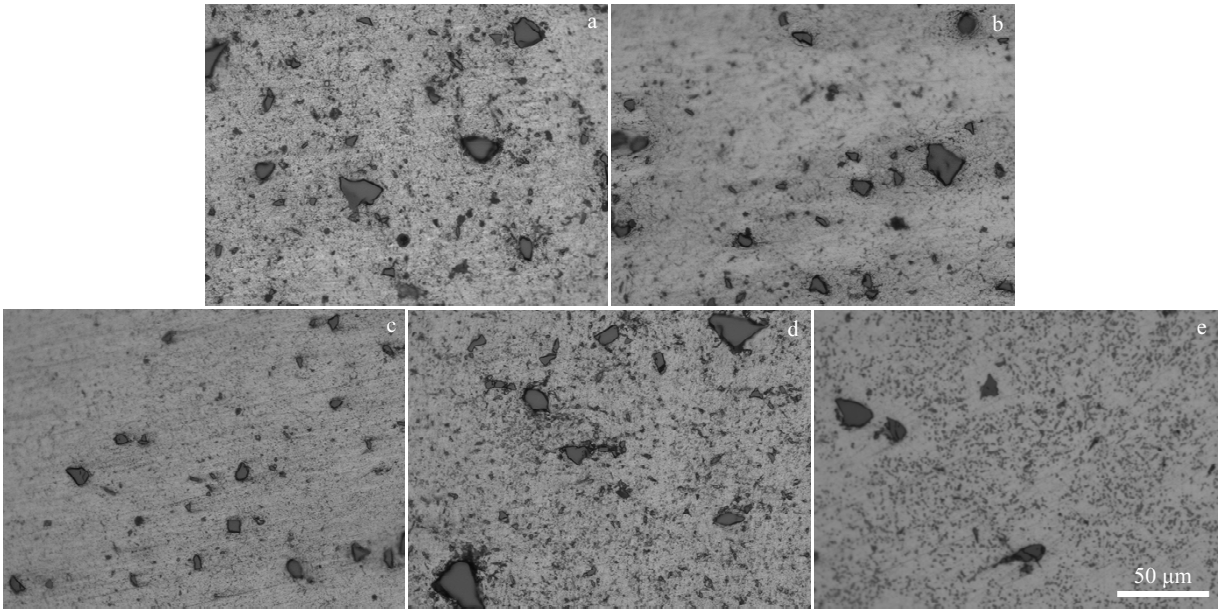

Fig.5 OM images of as-sintered samples containing 7vol%B_4C-4.67vol%Ti (a), 5vol%B_4C-3.33vol%Ti (b), 3vol% B_4C-2vol%Ti (c), 5vol% B_4C (d), and 3vol% B_4C (e)

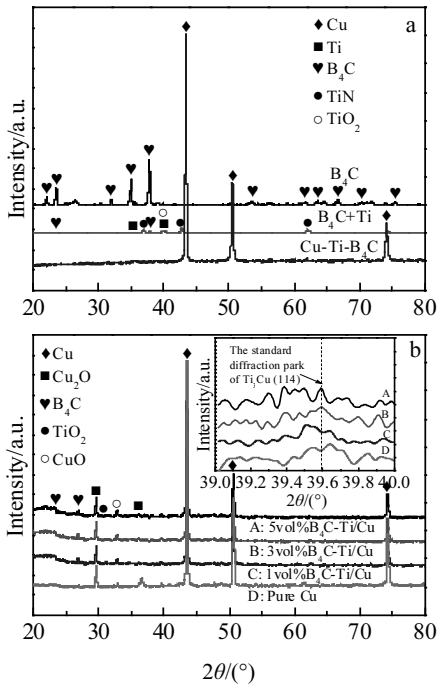

Fig.6 XRD patterns of as-received and ball milled powder (a) and as-SPSed CTBCs and bulk Cu (b)

Fig.6b shows the XRD patterns of sintered CTBCs as a function of (B_4C+Ti) volume fraction. Apart from the presence of primary peaks corresponding to Cu and B_4C in the composite, most of the additional peaks correspond to the reaction products of copper or titanium and adsorbed gas. Particularly, because of the high reactivity of nano-Ti and the intense oxytropic character of Cu, these compounds are formed in the fabrication process. Recently, the reaction system between B_4C and Ti has been widely reported based on the following equation[16]:

$$3Ti + B_4C \rightarrow 2TiB_2 + TiC \quad (1)$$

At 700 °C, the change in Gibbs free energy value for the chemical reaction is calculated to be –642.24 kJ·mol^{-1}. In the present work, no new additional interfacial products (like TiB_2 and TiC phases) were presented in the CTBCs (Fig.6b, XRD patterns), which may be due to the relatively low content of these phases. Additionally, Ti_3Cu intermetallic phases emerge on the Cu/Ti interface of CTBCs proved by XRD analysis, which indicates a diffusion bonding between (B_4C+Ti) particle and the copper matrix.

Fig.7a shows the SEM-EDS line scanning position on the sintered sample and the variations of element content along the straight line are displayed in Fig.7b. The brighter background is the Cu matrix while the dark oval areas represent the (B_4C+Ti) coated particles. Thus, the titanium content is high at the reinforcement zone and tends to evolve toward the matrix zone through the smooth transition layer (Fig.7b). Simultaneously, the distribution of Cu element decreases gradually from the side of Cu matrix to the side of Ti interlayer, which could infer the formation of metallurgical bonding at the interface of CTBCs. As can be seen, this is a good interfacial bonding between micro-B_4C/nano-Ti particulates and the Cu-matrix. Furthermore, the oxygen content is high at the Ti interlayer due to the high specific surface area of nano-Ti powders and its tremendous reactivity

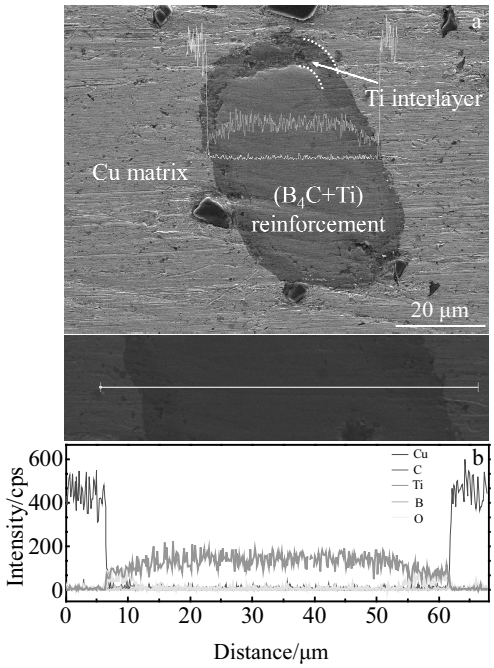

Fig.7 SEM image (a) and EDS line scanning (b) of 3vol% B_4C-2vol% Ti/Cu sample

with oxygen, which possibly makes compounds (TiO_2 etc.) be generated at the bonding interfaces. It might make impact on interfacial bonding strength to some extent. Also, EDS mapping in Fig.8 shows the elemental distribution of CTBCs. The diffusion of the elements could be observed near the interface from Fig.8b~8e. This is not only conducive to improving the reinforcement/matrix interface bonding but would also enhance the interfacial strengthening effectively.

2.2 Relative density and hardness measurements

The theoretical density, measured density and relative density of as-SPSed samples are listed in Table 1. As it can be seen, the theoretical density of CTBCs decreases as the (B_4C+Ti) particulate volume fraction increases. It is due to the lower density of the coated ceramic particulates than that of the Cu-matrix. The measured density of the samples exhibits the similar trend with theoretical density with increasing the (B_4C+Ti) particulate contents. However, the highest relative density (97.27%) is revealed by the 3vol%B_4C-2vol%Ti/Cu sample. Generally, an increasing content of hard ceramic phase causes an increase in the micropore volume because of the sharp edges and little plastic deformation of B_4C particles. By comparison, uncoated B_4C/Cu specimens have lower relative density at the same B_4C contents, which indicates that the refinement of particulate size is beneficial to reducing the porosity of Cu-composites, as discussed earlier. Further, the densification mechanism of the monolithic CTBCs is attributed to: (i) the growth and bonding of sintering neck formed in the particle-particle contact area, (ii) the presence of arc discharge behavior, which is generated in the contact points between the powder particulates during sintering, and (iii) the constant self-heating effect based on the Joule heat theory[17].

Fig.9 shows microhardness values of the as-SPSed samples with and without the coated particles. It indicates that hardness of Cu-composites are improved with the increase in reinforcement percentage. When the (B_4C+Ti) particle content is 7 vol%, the microhardness value of the specimen reaches the highest, with an increase of 45% compared to that of pure Cu. The improved micro-hardness can be attributed to the higher

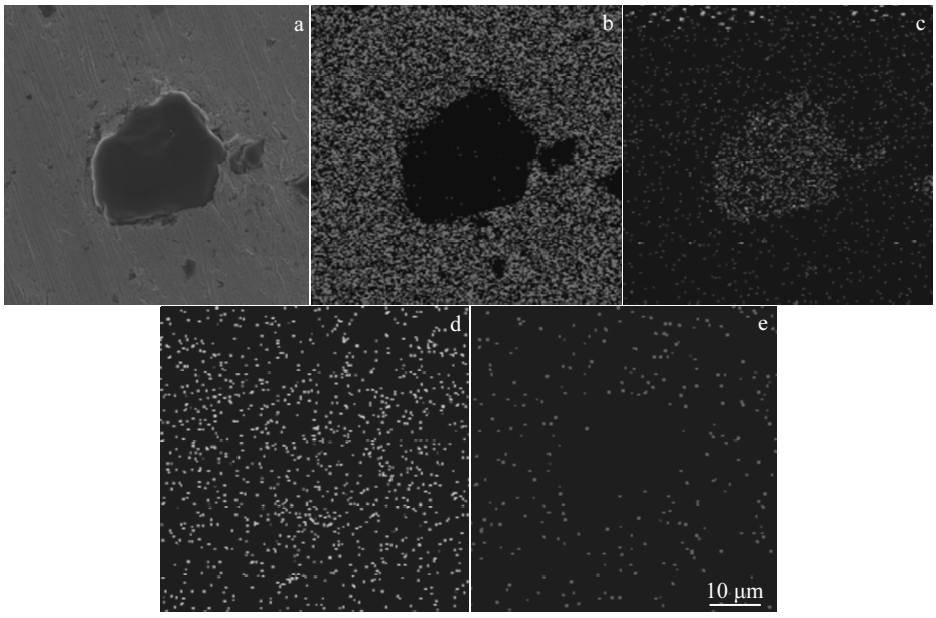

Fig.8 SEM image (a) and EDS mapping of CTBCs sample of 3vol% B_4C-2vol% Ti/Cu: (b) Cu, (c) B, (d) C, and (e) Ti

Table 1 Density of as-SPSed Cu-composites

Material	Theoretical density/ g·cm^{-3}	Measured density/ g·cm^{-3}	Relative density/ %
Pure Cu	8.91	8.39	94.24
3vol%B_4C-2vol%Ti/Cu	8.62	8.38	97.27
5vol%B_4C-3.33vol%Ti/Cu	8.43	8.00	94.93
3vol%B_4C/Cu	8.71	8.40	96.44
5vol%B_4C/Cu	8.58	8.11	94.55

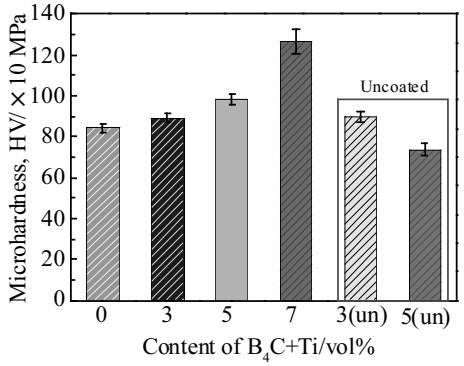

Fig.9 Hardness variations versus reinforcement contents in the as-SPSed Cu-composites

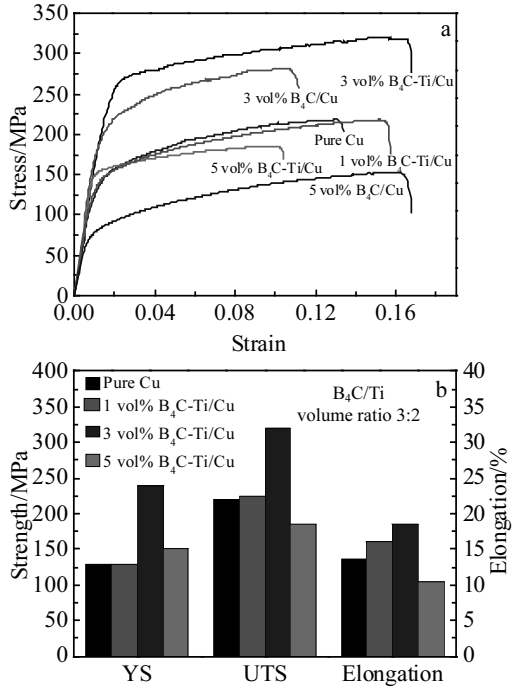

Fig.10 Tensile stress-strain curves (a) and the variation of tensile properties of the CTBCs with different volume fractions of reinforcement (b)

bearing capacity offered by the hard ceramic particles towards local Cu matrix deformation under indentation and the rising of dislocation density due to the addition of (B_4C+Ti) particulates together with other intermetallic compounds, which resists the dislocation movement in the matrix. Furthermore, the refinement of the grain size of copper matrix during SPS is partly beneficial to the enhancement of mechanical property. Compared to the CTBCs, it is obvious that the uncoated B_4C/Cu composites exhibit lower microhardness values because of the enlarged porosity. Accordingly, the microhardness revealed is correlated with the relative density to some extent.

2.3 Mechanical properties

Fig.10a shows the tensile stress-strain curves of pure Cu and composite samples fabricated by SPS. The variations of the yield strength (σ_{YS}), ultimate tensile strength (σ_{UTS}) and elongation to fracture versus (B_4C+Ti) content are displayed in Fig.10b. As can be seen, all performance indexes of the CTBCs initially increase with increasing the (B_4C+Ti) reinforcement contents from 0 vol% to 3 vol% and later decrease from 3 vol% to 5 vol%. The 3 vol%B_4C-Ti/Cu composites exhibit a combination of the highest strengths and elongation. Further, the UTS strength of CTBCs is increased to 320 MPa from 220 MPa, or by 45% increment in comparison to that of pure Cu matrix prepared by an identical processing method (SPS). Simultaneously, the developed CTBCs possess an excellent deformability (18.5% of elongation of 3 vol%B_4C-Ti/Cu). In general, the yield strength increases directly in proportion to the volume fraction of the reinforcement particulates. However, the YS of 5 vol%B_4C-Ti/Cu exhibits the poorer strength, mainly due to the inadequate densification. Thus, the tensile property of the high-content CTBCs has huge potential to be improved by subsequent hot deformation such as extrusion and rolling. Based on the results of tensile testing, it is concluded that mechanical properties of the uncoated B_4C/Cu composites have not been enhanced significantly compared with the superior CTBCs, which could be due to the absence of good interface bonding between the matrix and the reinforcement.

Generally, the tensile strength of CTBCs may be enhanced by the following strengthening mechanisms:

(a) The presence of uniformly distributed hybrid reinforcement ((B_4C+Ti) particulate and little intermetallics) phases and the effective load transfer from Cu matrix to (B_4C+Ti) particulate, which depends on the superior interfacial bonding strength. It could be calculated with the following equation[18]:

$$\Delta\sigma_{\text{Load}} = \frac{1}{2}\sigma_{\text{ym}}V_{\text{f}} \quad (2)$$

where, σ_{ym} is the yield strength of Cu matrix and V_{f} is volume fraction of the (B_4C+Ti) reinforcement. The increase of V_{f} results in the increase of $\Delta\sigma_{\text{Load}}$.

(b) The grain refinement because of the addition of nano-titanium particulate into Cu matrix, as well as the formation of small grain size during the rapid SPS process[19-21]. The grains refinement effect in CTBCs can be described via the well-known Hall-Petch equation which is expressed as:

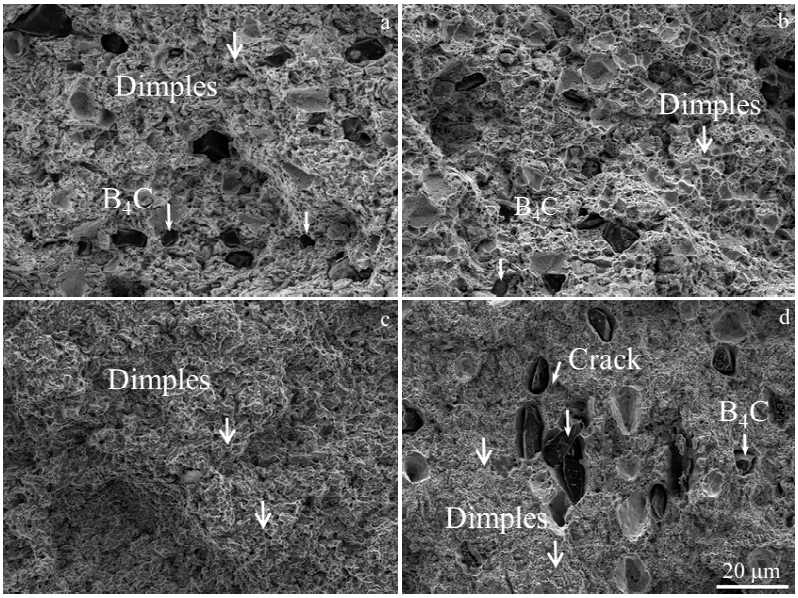

Fig.11 SEM fractographs of 5vol%B_4C-Ti/Cu (a), 3vol% B_4C-Ti/Cu (b), pure Cu (c), and 5vol%B_4C/Cu (d)

$$\sigma_{YS} = \sigma_0 + K_y d^{-1/2} \quad (3)$$

where σ_0 and K_y are constants and d is the average grain size. It is clear that the yield strength is inversely proportional to grain size[22].

(c) When CTBCs undergo temperature variation, coefficient of thermal expansion (CTE) mismatch between the Cu matrix and the hybrid (B_4C+Ti) reinforcements (Cu is 17.6×10^{-6} K^{-1}, Ti is 11.1×10^{-6} K^{-1} and B_4C is 5.7×10^{-6} K^{-1}) would result in CTE mismatch strain at the reinforcement/matrix interface and enhancement of dislocation density in the copper matrix, which will improve the strength. Indeed, CTE mechanism plays a critical role in contributing to the strengthening effect in CTBCs. It can be given as:

$$\Delta\sigma_{CTE} = \sqrt{3}\varphi G_m b\left[\frac{12V_f\Delta\alpha\Delta T}{b(1-V_f)d_p}\right]^{1/2} \quad (4)$$

where, φ is the strengthening coefficient, G_m is the shear modulus of Cu matrix, b is the Burger vector, V_f is the volume fraction of the reinforcement, $\Delta\alpha$ is the difference in the coefficients of the thermal expansion, ΔT represents the difference between the sintering and room temperatures and d_p is the particle size.

Considering the particulate size and content of (B_4C+Ti) hybrid reinforcement, the effect of Orowan strengthening mechanism may be unremarkable. Importantly, the all above-mentioned contributions are predicted to make the simultaneous impact on CTBCs[23].

The results of fractographic analysis carried out on the fractured specimens of Cu-composites under tensile testing are shown in Fig.11. As shown in Fig.11a and 11b, there exist many large, deep and uniformly distributed dimples at the fracture surface of CTBCs, which belong to the typical ductile fractures. As is known, both size and depth of dimples are determined by the ductility and toughness of the composites. Hence, CTBCs exhibit excellent deformability of matrix. In the case of pure Cu, a number of dimples are visible in the sample; however, their sizes are smaller than those of CTBCs. In contrast, micro-cracks and voids are observed in the vicinity of the uncoated B_4C particulate for B_4C/Cu composite (in Fig.11d). This is due to the fact that the crack generated at the reinforcement/matrix interface becomes wider as the tension deformation increases[24]. In this case, the plastic failure of copper matrix plays an important role in the fracture behavior of the B_4C/Cu composites.

3 Conclusions

1) Copper matrix composites that contain micro-B_4C/nano-Ti hybrid reinforcements may be fabricated by combining both HEBM and SPS processing routes.

2) The as-SPSed 3 vol% B_4C-Ti/Cu composites exhibit the best combination of properties with enhanced strength and retained ductility. Microhardness, YS, UTS and elongation of the 3 vol% CTBCs are increased by 6%, 86%, 45% and 37%, respectively compared with those of pure Cu matrix.

3) The remarkable improvement in the mechanical properties of CTBCs can be attributed to: (i) the uniform distribution of (B_4C+Ti) reinforcements and (ii) the good interface bonding between Cu matrix and coated B_4C particulates.

References

1 Guo M X, Yi L, Zhu J *et al. Materials Characterization*[J], 2016, 120: 109

2 Wu K, Deng K K, Nie K B *et al. Materials & Design*[J], 2010, 31(8): 3929
3 Hou F L, Ni F, Cui Y S *et al. Rare Metal Materials and Engineering*[J], 2011, 40(12): 2175 (in Chinese)
4 Bagheri G H A. *Journal of Alloys and Compounds*[J], 2016, 676: 120
5 Tushar B, Soumya N, Ren Y *et al. Journal of Alloys and Compounds*[J], 2014, 617: 933
6 Geng J W, Hong T R, Ma Y *et al. Materials & Design*[J], 2016, 98: 186
7 Chellvarajoo S, Abdullah M Z, Khor C. *Materials & Design*[J], 2015, 82: 206
8 Sankaranarayanan S, Sabat R K, Jayalakshmi S *et al. Materials Chemistry and Physics*[J], 2014, 143(3): 1178
9 Wu Haixin, Ge Changchun, Yan Qingzhi *et al. Materials Science and Engineering A*[J], 2017, 699: 156
10 Menapace C, Cipolloni G, Hebda M *et al. Powder Technology*[J], 2016, 291: 170
11 Froumin N, Frage N, Aizenshtein M *et al. Journal of the European Ceramic Society*[J], 2003, 23(15): 2821
12 Patidar Dinesh, Rana R S. *Materials Today: Proceedings*[J], 2017, 4(2): 2981
13 Zhu Y D, Yan M F, Zhang Y X *et al. Computational Materials Science*[J], 2016, 123: 70
14 Li G L, Jiang X C, Wen M *et al. Journal of Materials Engineering*[J], 2001, 8: 32 (in Chinese)
15 Radune M, Zinigrad M, Kalabukhov S *et al. Ceramics International*[J], 2016, 42(9): 11 077
16 Tabrizi S G, Sajjadi S A, Babakhani A *et al. Journal of Alloys and Compounds*[J], 2017, 692: 734
17 Chen H S, Wang W X, Li Y L *et al. Materials & Design*[J], 2016, 94: 360
18 Chelliah N M, Singh H, Raj R *et al. Materials Science and Engineering A*[J], 2017, 685: 429
19 Feng H B, Zhou Y, Jia D C *et al. Material Science and Technology*[J], 2003, 11(3): 329 (in Chinese)
20 Fang Q, Kang Z X, Gan Y W *et al. Materials & Design*[J], 2015, 88: 8
21 Li H X, Song K X, Zhang Y M *et al. Hot Working Technology*[J], 2013, 42(24): 2 (in Chinese)
22 Byung-Wook Ahn. *Journal of Alloys and Compounds*[J], 2017, 693: 688
23 Gupta R K, Fabijanic D, Dorin T *et al. Materials & Design*[J], 2015, 84: 270
24 Qin L, Wang J, Wu Q *et al*. *Journal of Alloys and Compounds*[J], 2017, 712: 69

含微纳 B_4C/Ti 颗粒铜基复合材料的微观组织与力学性能

安德成，王文先，陈洪胜，谭敏波，王 苗
(太原理工大学 先进镁基材料山西省重点实验室，山西 太原 030024)

摘 要：采用高能球磨(HEBM)和放电等离子烧结(SPS)工艺成功制备出微纳 B_4C/Ti 颗粒增强铜基复合材料(CTBCs)，通过 X 射线衍射(XRD)、光学显微镜(OM)、扫描电子显微镜(SEM)以及能谱(EDS)等测试手段对其微观组织形貌进行表征，并测定了烧结态试样的致密度和力学性能。结果表明，(B_4C+Ti)颗粒在基体中均匀分布，增强体与铜基体界面结合良好，且其结合形式为冶金结合和机械结合并存。复合材料的显微硬度、拉伸屈服强度、抗拉强度和延伸率等力学性能相较于纯铜试样得到显著提高，这主要归因于载荷传递、细化晶粒与热错配等强化机制。复合材料的拉伸断口表现出明显的韧性断裂特征。

关键词：铜基复合材料；放电等离子烧结；高能球磨；界面结合；力学性能

作者简介：安德成，男，1994 年生，博士生，太原理工大学材料科学与工程学院，山西 太原 030024，电话：0351-6010076，E-mail: adc994@126.com